Exploring *Andrographis paniculata* Phytochemicals for Allosteric Modulation of Mycobacterial Isocitrate Lyase 2: Implications for TB Preventive Therapy

Shreya Roy and, Vibha Gupta*

Department of Biotechnology, Jaypee Institute of Information Technology, A -10 Sec 62, Noida

Email: 23401007@mail.jiit.ac.in and vibha.gupta@jiit.ac.in * Corresponding author

Abstract

Tuberculosis (TB), caused by *Mycobacterium tuberculosis* (Mtb), remains a major global health burden due to its ability to persist in a latent drug-tolerant state. During latency, Mtb relies on host lipids and activates the glyoxylate shunt to bypass carbon-loss steps of the tricarboxylic acid cycle. This pathway is driven by isocitrate lyase (ICL), present as two isoforms, ICL1 and ICL2. While ICL1 functions as the primary catalytic enzyme, ICL2 contains a distinct C-terminal regulatory Domain IV where acetyl-CoA binds and allosterically enhances enzymatic activity, promoting lipid-dependent persistence. Given that this regulatory pocket is structurally independent of the catalytic center, it offers a selective target for allosteric inhibition of the persistent-associated factor.

Phytochemicals from *Andrographis paniculata* (Kalmegh), a plant known for antimycobacterial activity, were therefore investigated as potential modulators of ICL2. Molecular docking against the acetyl-CoA–binding Domain IV, followed by *in silico* ADMET and ProTox-3 toxicity prediction, identified candidates capable of interfering with acetyl-CoA–mediated activation. Notably, several plant-derived bioactives exhibited higher predicted binding affinity than acetyl-CoA at the regulatory pocket across both open and closed conformational states, along with favourable pharmacokinetic and toxicity profiles. These findings support allosteric targeting of ICL2 as a structurally informed strategy to disrupt lipid-dependent persistence and provide candidate scaffolds for future anti-latency therapeutic development.

Keywords: *Mycobacterium tuberculosis*, Isocitrate lyase (ICL2), *Andrographis paniculata*, Kalmegh, Phytocompounds

Introduction

Tuberculosis (TB), caused by *Mycobacterium tuberculosis* (Mtb), remains a leading cause of infectious mortality worldwide[1]. A major challenge in TB control is latent tuberculosis infection (LTBI), in which bacteria persist in a non-replicating, drug-tolerant state within host tissues [2]. Current preventive therapy guidelines therefore recommend treatment of high-risk groups, particularly household contacts of TB-infected patients and immunocompromised individuals, with one or more anti-TB drugs to prevent progression to active disease.

During latency, Mtb relies predominantly on host-derived lipids as carbon sources, necessitating metabolic reprogramming that bypasses the decarboxylative steps of the tricarboxylic acid (TCA) cycle [3]. This metabolic adaptation is mediated by the glyoxylate shunt, in which isocitrate lyases catalyze the cleavage of isocitrate into glyoxylate and succinate, conserving carbon for gluconeogenesis and supporting long-term persistence[4]. Despite the essential role of this pathway in persistence and virulence, no clinically approved inhibitor targeting the glyoxylate shunt is currently available.

The Mtb genome encodes two isocitrate lyase isoforms, ICL1 and ICL2, both of which contribute to the pathogen's lipid-dependent survival within granuloma lesions. ICL1 has been extensively characterized structurally and biochemically and has been the primary focus for most inhibitor development efforts[5] . In contrast, ICL2 remains relatively understudied, largely because its three-dimensional crystal structure was resolved only in 2019. The recent structural elucidation, however, has revealed a distinct C-terminal allosteric domain that binds acetyl-CoA and enhances ICL2's enzymatic activity. Structural studies of the apo and acetyl-CoA–bound forms demonstrate that acetyl-CoA binds specifically within domain IV, with residues Arg493, Lys497, His500, Arg505, and Ser509 [6]. Ligand binding induces conformational rearrangement of the C-terminal tail (residues 485–520), reorganizes inter-subunit interactions, and converts the enzyme from an open, flexible tetramer to a compact, closed conformation. This structural transition stabilizes regions adjacent to the catalytic site and improves substrate positioning, thereby enhancing isocitrate lyase activity during lipid-dependent persistence [5], [6]. So, in this study, both open and closed conformations of ICL2 were analyzed to account for the conformational changes induced by acetyl-CoA binding and to assess potential regulation via competitive or allosteric

mechanisms. Since Domain IV is spatially distinct from the catalytic cleft, targeting this region allows inhibition of enzymatic activation without directly competing with substrate binding.

Building on this structural insight, phytochemicals from *Andrographis paniculata* (Kalmegh), known for their antimycobacterial activity [7], were evaluated for their potential to interfere with acetyl-CoA binding to Domain IV of ICL2. Structure-based *in silico* docking was followed by ADMET profiling and ProTox-3 toxicity prediction to shortlist the candidate compounds capable of disrupting acetyl-CoA–mediated activation, thereby impairing ICL2 function and persistence in latent Mtb. These candidate inhibitors may represent a selective strategy to prevent enzyme activation, suppress persistence-associated metabolism, and potentially strengthen tuberculosis preventive therapy.

2. Materials and Methods

2.1. Molecular Docking

Phytochemicals from Kalmegh were retrieved from the IMPPAT database [8]. Structures were downloaded in SDF format and converted to PDBQT format using Open Babel.

The crystal structures of Mtb ICL2 (CDC1551) in open (PDB ID: 6EDW) and closed (PDB ID: 6EE1) conformations were downloaded from the Protein Data Bank. Protein preparation was performed using AutoDock Tools by removing water molecules, adding polar hydrogens, assigning Kollman charges, and converting the structures to PDBQT format [9].

Docking was carried out using AutoDock Vina. Two binding sites were targeted: (i) the acetyl-CoA regulatory domain (Domain IV) to identify potential allosteric inhibitors, and (ii) the catalytic active site to assess interactions at the substrate-binding pocket. Grid boxes were centered on the respective binding regions to encompass key interacting residues. Docking poses of ligand were ranked based on binding affinity (kcal/mol) and interaction patterns.

2.2. ADME Analysis

Pharmacokinetic and drug-likeness properties of the compounds were predicted using SwissADME [10]. SMILES of all compounds were submitted to evaluate absorption, distribution, metabolism, excretion, solubility, and compliance with Lipinski's rule of five.

2.3. Toxicity Prediction

In silico toxicity profiling was performed using ProTox-3 [11]. Compounds were assessed for hepatotoxicity, cardiotoxicity, neurotoxicity, mutagenicity, and carcinogenicity. Only compounds with favourable toxicity profiles were considered as potential ICL2 inhibitors.

3. Results and discussions

3.1 Compound Selection and Characterization

A total of 77 phytochemicals were initially retrieved from the IMPPAT database. Manual curation was performed to remove entries with duplicate IMPHY IDs and identical SMILES, resulting in a final set of 27 Kalmegh bioactive molecules for further analysis. These compounds span diverse phytochemical classes, including flavonoids, diterpenoids, phenolic acids, indole derivatives, terpenoid lactones, and fatty acids, reflecting the rich chemical diversity of Kalmegh (Table 1). The molecular weights of the selected compounds ranged from 150.22 g/mol (Carvacrol) to 536.48 g/mol (Andrographidine F), with most compounds falling within the drug-like range (<500 g/mol). Structurally, diterpenoid lactones such as andrographolide and its derivatives formed the characteristic scaffold of Kalmegh bioactives, defined by a bicyclic diterpene core with lactone functionality and multiple hydroxyl substitutions. Flavonoid glycosides, including andrographidine variants, exhibited polyphenolic frameworks with sugar moieties contributing to polarity and hydrogen bonding potential. Other naturally occurring metabolites such as chlorogenic acid, indole derivatives, and fatty acids provided additional structural diversity and provided a suitable chemical space for evaluating interactions with both catalytic and allosteric regions of ICL2.

Table 1: Phytochemical classification of the compounds.

S.No	Compound	MW (g/mol)	Phytochemical Class
1	14-Deoxy-12-methoxyandrographolide	364.48	Diterpenoid
2	14-Deoxyandrographolide	334.45	Diterpenoid
3	5-Hydroxy-7,8-dimethoxyflavone	298.29	Flavonoid

4	Andrographidine B	492.43	Flavonoid glycoside
5	Andrographidine C	460.43	Flavonoid glycoside
6	Andrographidine D	520.48	Flavonoid glycoside
7	Andrographidine E	490.46	Flavonoid glycoside
8	Andrographidine F	536.48	Flavonoid glycoside
9	Andrographidin A	462.45	Flavonoid glycoside
10	Andrographin	328.32	Flavone
11	Andrographiside	512.59	Diterpenoid glycoside
12	Andrograpanin	318.45	Diterpenoid
13	Andropanoside	496.59	Diterpenoid glycoside
14	Apigenin	270.24	Flavone
15	Carvacrol	150.22	Phenolic monoterpene
16	Chlorogenic acid	354.31	Phenolic acid
17	Deoxyandrographolide	334.45	Diterpenoid
18	Eugenol	164.2	Phenylpropanoid phenol
19	Indole-3-carboxylic acid methyl ester	175.18	Indole derivative
20	Myristic acid	228.37	Fatty acid
21	Oroxylin A	284.26	Flavone
22	Paniculide A	264.32	Terpenoid lactone
23	Paniculide B	280.32	Terpenoid lactone
24	Paniculide C	278.3	Terpenoid lactone
25	Skullcapflavone I	314.29	Flavonoid
26	Tetramethoxyflavone	358.34	Polymethoxyflavone
27	Wogonin	284.26	Flavone

3.2 Structural Basis for Targeting the Allosteric Domain of ICL2

The crystal structures of Mtb ICL2 (PDB IDs: 6EDW – open conformation; 6EE1 – acetyl-CoA–bound closed conformation) enabled structure-guided docking analysis and comparative evaluation of regulatory and catalytic binding sites.

3.2.1 Docking at the Acetyl-CoA binding Domain IV

Phytochemicals from Kalmegh were docked at the acetyl-CoA regulatory Domain IV of both open and closed Mtb ICL2 structures. For the closed conformation (PDB ID: 6EE1), the grid box was defined with dimensions of 64 × 50 × 46 points, a spacing of 0.375 Å, and centered at (−31.403, 106.513, 32.846) for the Domain IV binding site. For the open conformation (PDB ID: 6EDW), the grid box was set to 60 × 102 × 56 points with the same spacing (0.375 Å) and centered at (48.574, 73.731, 3.460). Acetyl-CoA was used as a reference cutoff for screening, with docking scores of −7.3 kcal/mol in the open structure and −8.6 kcal/mol in the closed structure. *In-silico* docking of kalmegh bioactives reveal multiple compounds with better binding affinities than acetyl-CoA in both conformations (Table 2).

Table 2: Docking score of top 5 compounds at the acetyl-CoA binding domain of *Mtb* CDC1551 ICL2 in open (PDB ID:6EDW) and closed (PDB ID: 6EE1) confirmations.

Rank	**Compound Name**	**Docking score in open structure (kcal/mol)**	**Docking score in closed structure (kcal/mol)**
Control	**Acetyl co-A**	**-7.3**	**-8.6**
1	Andrographidine E	-7.8	-9.7
2	Andrographiside	-8	-9.2
3	Andrographidin A	-7.9	-8.7
4	Chlorogenic acid	-7.2	-8.6
5	Andrographidine B	-8.2	-8.5

3.2.2 ADME and Toxicity Prediction

The shortlisted five Kalmegh phytochemicals at the acetyl-CoA binding site of ICL2 were assessed for pharmacokinetic properties using SwissADME (Table 3), and all compounds demonstrated favourable drug-like characteristics with 0–2 Lipinski violations. Lipinski's rule of five was considered without strict exclusion, since previous studies including Shabnashmi et al. (2020) and Thai et al. (2025) on *Andrographis paniculata* compounds, have shown that bioactive phytochemicals frequently fall outside classical Lipinski criteria while retaining significant therapeutic potential. Their structural complexity and functional diversity contribute to target specificity and biological activity, making minor Lipinski violations acceptable at this stage and not limiting their progression for further optimization or alternative delivery strategies.

Table 3: ADME profile of top 5 compounds.

S. No	Compound	H-bond donor	H-bond acceptor	Rotatable bonds	TPSA (Å²)	LogP	LogS	Lipinski Violations
1	Andrographidine E	7	11	4	121.54	0.38	-3.34	1
2	Andrographiside	6	10	6	127.6	0.81	-2.63	2
3	Andrographidin A	6	10	4	112.63	0.43	-3.01	0
4	Chlorogenic acid	5	9	6	83.5	-0.75	-1.62	1
5	Andrographidine B	6	12	6	119.1	0.35	-3.34	2

ProTox-3 analysis of the top five Kalmegh phytochemicals (Table 4) revealed that Chlorogenic acid and Andrographidine B exhibited a complete absence of predicted toxicity across hepatotoxicity, neurotoxicity, cardiotoxicity, carcinogenicity, and BBB permeability, with LD_{50} values of 5000 mg/kg (Class 5). In contrast, the other three compounds showed at least one predicted toxicity, such as cardiotoxicity or BBB activity. These results highlight Chlorogenic acid and Andrographidine B as the safest candidates for further evaluation and rational prioritization as potential lead molecules for ICL2 inhibition.

Table 4: ProTox- 3 analysis of top 5 compounds.

S. No	Compound	Hepatotoxicity	Neurotoxicity	Cardiotoxicity	Carcinogenicity	BBB Permeability	Predicted LD_{50} in mg/Kg (Toxicity class)
1	Andrographidine E	Inactive	Inactive	Active	Inactive	Active	5000(5)
2	Andrographiside	Inactive	Inactive	Active	Inactive	Inactive	590(4)
3	Andrographidin A	Inactive	Inactive	Active	Inactive	Inactive	3000(5)
4	Chlorogenic acid	Inactive	Inactive	Inactive	Inactive	Inactive	5000(5)
5	Andrographidine B	Inactive	Inactive	Inactive	Inactive	Inactive	5000(5)

3.3 Binding Mode Comparison Between Closed (6EE1) and Open (6EDW) Conformations

All the listed compounds contain multiple hydroxyl groups and extended aromatic systems demonstrating enhanced complementarity to the polar and partially charged environment of Domain IV. These phytochemicals occupy the acetyl-CoA–binding pocket (in both open and closed confirmations) and form hydrogen-bonds as well as electrostatic interactions with key acetyl-CoA binding residues Arg493, Lys497, His500, Arg505, and Ser509 of domain IV. To delineate how ligand binding influences conformational stabilization of Domain IV, interaction profiles were compared between the open (6EDW) and acetyl-CoA–bound closed (6EE1) structures of Mtb ICL2. In the open conformation (6EDW), ICL2 forms an A–B dimeric interface in which acetyl-CoA engages a network

of polar and charged residues, including Arg550, Arg553, Arg674, Arg699, Glu640, Glu605, Gln663, Gln635, and Ser639. In the closed conformation (6EE1), domain rearrangement results in an A–C dimer configuration, with acetyl-CoA interacting primarily with Arg264, Arg409, Asp418, Asp422, Glu242, and Glu424, in addition to nearby hydrophobic residues Trp421, Cys423, and Leu405. Although residue numbering differs due to domain movement and chain reassignment, spatial alignment confirms that these residues occupy structurally equivalent positions. This conservation indicates that the geometry of acetyl-CoA recognition is preserved despite global conformational reorganization. Comparative ligplots displayed in Figure 1 exhibit conformational adaptability between the two states. In the open structure of ICL2, Andrographidine B binding interaction is majorly polar in nature with hydrogen bonding with Arg699, Glu640, Gly638, Ser639, and Gln663. In contrast, within the closed conformation, hydrophobic contacts involving Arg699, Arg608, Leu642, Phe700, and Thr669 became more prominent. This interaction shift suggests that andrographidine B preferentially stabilizes the compact regulatory pocket characteristic of the activated tetramer, potentially interfering with acetyl-CoA–mediated structural consolidation. Similar positional variability is demonstrated by Chlorogenic acid where it interacts with Lys686, Arg687, Thr690, Gln685, and Gln676 in 6EDW (open state), but shifts toward residues Arg665, Gly416, Phe381, Val378, and Glu387 in 6EE1 (closed state). This relocation indicates a change in binding microenvironment rather than preservation of a conserved regulatory interaction geometry. Collectively, these observations indicate that multiple bioactives of kalmegh maybe effective competitive or allosteric modulators of domain IV ICL2.

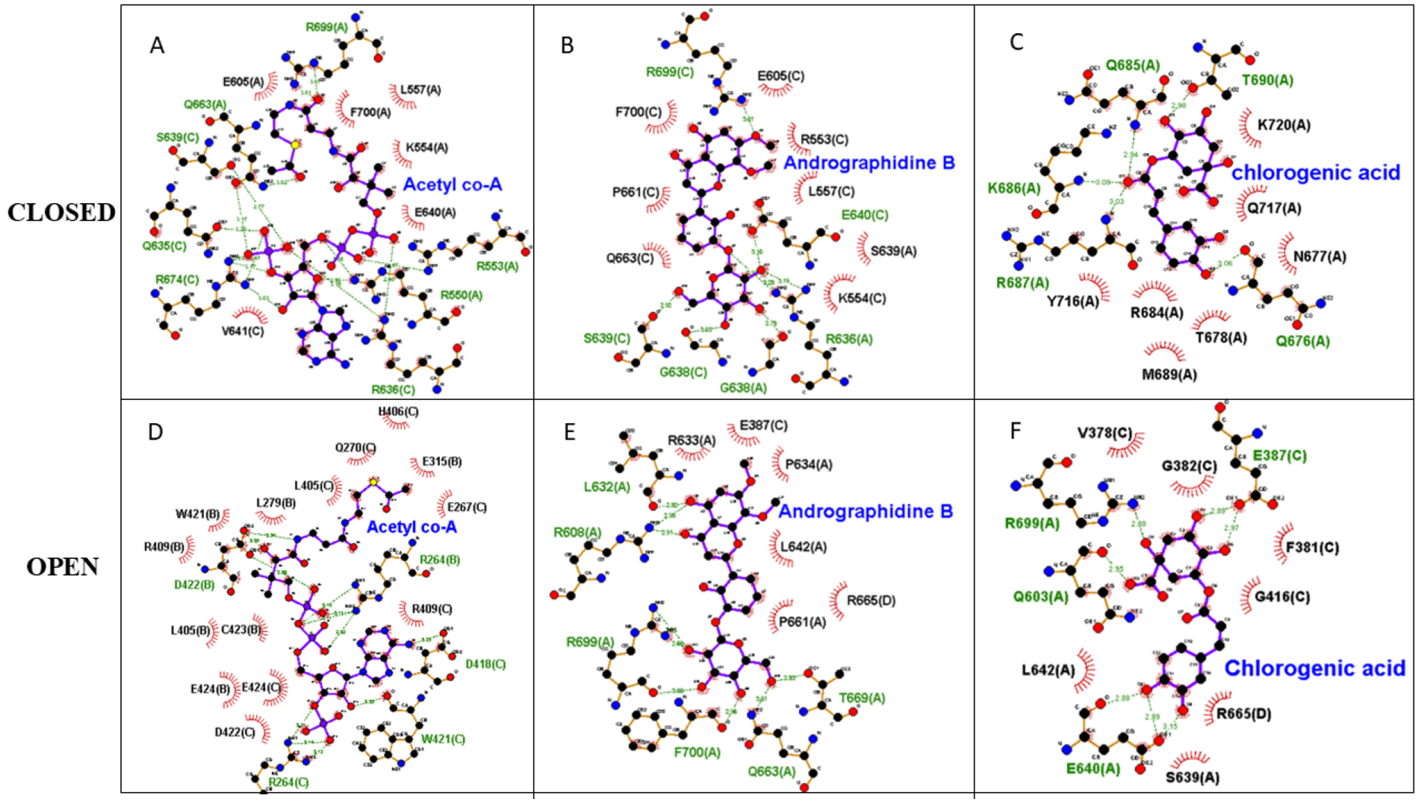

Figure 1- Ligplot interaction at the acetyl-CoA binding site of *Mycobacterium tuberculosis* CDC1551 ICL2: (A) acetyl-CoA, (B) andrographidine B and (C) chlorogenic acid in the closed conformation (PDB:6EE1) and the same ligands (D-F) in the open conformation (PDB: 6EDW)

This study adopted a structure-guided, persistence-oriented strategy by targeting the acetyl-CoA–binding regulatory domain of mycobacterial ICL2, a site directly implicated in metabolic adaptation during latent infection. Phytochemicals from *Andrographis paniculata* were systematically screened to identify potential modulators capable of interfering with acetyl-CoA- mediated enzymatic activation. Among the evaluated compounds, Andrographidine B and Chlorogenic acid demonstrated stable occupancy of the regulatory pocket for both conformational states of ICL2, along with favourable pharmacokinetic parameters and low predicted

toxicity. Their interaction profiles suggest the potential to disrupt acetyl-CoA–induced conformational rearrangement of the tetramer, thereby attenuating ICL2 activity.

The results have clinical implications for selectively targeting latent Mtb through inhibition of ICL2, a key persistence factor, using Kalmegh phytocompounds. Latent Mtb relies on fatty-acid metabolism for long-term survival, and disruption of this allosteric regulatory mechanism offers a strategy distinct from conventional bactericidal drugs. Current tuberculosis preventive therapy primarily targets replicating bacilli and requires prolonged administration, whereas modulation of ICL2 activation could impair metabolic adaptation of dormant bacteria. This highlights the selective vulnerability of latent bacilli dependent on the glyoxylate shunt, with limited impact on actively replicating populations. Kalmegh derived compounds specifically Andrographidine B and Chlorogenic acid may target domain IV of ICL2 and may therefore serve as adjunct candidates for preventive therapy, but needs to be validated through experimental work.

References-

[1] T. K. Suvvari, “The persistent threat of tuberculosis − Why ending TB remains elusive?,” *J. Clin. Tuberc. Other Mycobact. Dis.*, vol. 38, p. 100510, Feb. 2025, doi: 10.1016/j.jctube.2025.100510.

[2] A. Egorova, E. G. Salina, and V. Makarov, “Targeting Non-Replicating Mycobacterium tuberculosis and Latent Infection: Alternatives and Perspectives (Mini-Review),” *Int. J. Mol. Sci.*, vol. 22, no. 24, p. 13317, Dec. 2021, doi: 10.3390/ijms222413317.

[3] J. E. Griffin *et al.*, “Cholesterol Catabolism by Mycobacterium tuberculosis Requires Transcriptional and Metabolic Adaptations,” *Chem. Biol.*, vol. 19, no. 2, pp. 218–227, Feb. 2012, doi: 10.1016/j.chembiol.2011.12.016.

[4] M. Antil and V. Gupta, “Lessons Learnt and the Way Forward for Drug Development Against Isocitrate Lyase from *Mycobacterium tuberculosis*,” *Protein Pept. Lett.*, vol. 29, no. 12, pp. 1031–1041, Dec. 2022, doi: 10.2174/0929866529666221006121831.

[5] V. Sharma *et al.*, “Structure of isocitrate lyase, a persistence factor of Mycobacterium tuberculosis,” *Nat. Struct. Biol.*, vol. 7, no. 8, pp. 663–668, Aug. 2000, doi: 10.1038/77964.

[6] R. P. Bhusal *et al.*, “Acetyl-CoA-mediated activation of Mycobacterium tuberculosis isocitrate lyase 2,” *Nat. Commun.*, vol. 10, no. 1, p. 4639, Oct. 2019, doi: 10.1038/s41467-019-12614-7.

[7] P. Bhatter, P. Gupta, P. Daswani, P. Tetali, and T. Birdi, “Antimycobacterial Efficacy of *Andrographis paniculata* Leaf Extracts Under Intracellular and Hypoxic Conditions,” *J. Evid. Based. Complementary Altern. Med.*, vol. 20, no. 1, pp. 3–8, Jan. 2015, doi: 10.1177/2156587214553303.

[8] K. Mohanraj *et al.*, “IMPPAT: A curated database of Indian Medicinal Plants, Phytochemistry And Therapeutics,” *Sci. Rep.*, vol. 8, no. 1, p. 4329, Mar. 2018, doi: 10.1038/s41598-018-22631-z.

[9] J. Eberhardt, D. Santos-Martins, A. F. Tillack, and S. Forli, “AutoDock Vina 1.2.0: New Docking Methods, Expanded Force Field, and Python Bindings,” *J. Chem. Inf. Model.*, vol. 61, no. 8, pp. 3891–3898, Aug. 2021, doi: 10.1021/acs.jcim.1c00203.

[10] A. Daina, O. Michielin, and V. Zoete, “SwissADME: a free web tool to evaluate pharmacokinetics, drug-likeness and medicinal chemistry friendliness of small molecules,” *Sci. Rep.*, vol. 7, no. 1, p. 42717, Mar. 2017, doi: 10.1038/srep42717.

[11] P. Banerjee, E. Kemmler, M. Dunkel, and R. Preissner, “ProTox 3.0: a webserver for the prediction of toxicity of chemicals,” *Nucleic Acids Res.*, vol. 52, no. W1, pp. W513–W520, Jul. 2024, doi: 10.1093/nar/gkae303.